Journal of Coastal Research	SI	33	223–236	West Palm Beach, Florida	Winter 2004

Medium-Term Bathymetric Change around Jetties at Imagireguchi Inlet, Japan

Yoshiaki Kuriyama*, Yusuke Uchiyama, Satoshi Nakamura*** and Tomokazu Nagae******

*Head, Littoral Drift Division
Marine Environment and Engineering Department
Port and Airport Research Institute
Nagase 3-1-1
Yokosuka, Kanagawa 239-0826, Japan
E-mail: kuriyama@pari.go.jp

**Senior Research Engineer
Marine Environment and Engineering Department
Port and Airport Research Institute
Nagase 3-1-1
Yokosuka, Kanagawa 239-0826, Japan

***Head, Sediment Environments Division
Marine Environment and Engineering Department
Port and Airport Research Institute
Nagase 3-1-1
Yokosuka, Kanagawa 239-0826, Japan

****Littoral Drift Division
Marine Environment and Engineering Department
Port and Airport Research Institute
Nagase 3-1-1
Yokosuka, Kanagawa 239-0826, Japan

ABSTRACT

KURIYAMA, Y.; UCHIYAMA, Y.; NAKAMURA, S., and NAGAE, T., 2003. Medium-term bathymetric change around jetties at Imagireguchi Inlet, Japan. *Journal of Coastal Research*, SI(33), 223–236. West Palm Beach (Florida), ISSN 0749-0208.

Medium-term bathymetric change induced by jetties at an entrance of a tidal inlet was examined with a 30-year bathymetric data set. Empirical orthogonal eigenfunction analysis and the investigation on volumetric change showed that the tidal channel deepened after construction of the jetties and that the erosion rate in the channel increased with time. The increase in the erosion rate is probably caused by the stabilization of the location of the channel and focusing of the ebb jet between the jetties. Although the accumulation rate on the up-drift side of the jetties decreased, the amount of sediment supplied to the down-drift beach did not increase. This is because some amount of sediment transported around the jetties was trapped by the ebb-tidal delta. The volume of sediment stored in the ebb-tidal delta was estimated, and compared with the equilibrium volume. Complex empirical orthogonal eigenfunction analysis showed that, during and just after construction of the jetties, shoals formed on both sides of the jetties and moved shoreward. Several years after the completion of construction, however, although the shoal on the down-drift side moved still shoreward, the shoal on the up-drift side moved seaward. The seaward movement of the shoal was assumed to be caused by the return flow and the wave-generated longshore current.

ADDITIONAL INDEX WORDS: *Tidal channel, ebb-tidal delta, shoal, empirical eigenfunction analysis, complex empirical eigenfunction analysis.*

INTRODUCTION

Jetties, constructed for the stabilization of navigation channels in many cases, trap sediments transported alongshore and cause bathymetric change on both sides of the inlet or entrance. Furthermore, jetties constructed at inlets have an influence on the complex inlet morphologic system including ebb-tidal deltas and tidal channels.

TOMLINSON (1991) investigated the development of an ebb-tidal delta and morphological changes of adjacent beaches after extension of jetties at the entrance of the Tweed River, a tidal river in Australia, where the mean spring tidal range is 0.9 m, and the tidal prism is about 13.5 $\times$ 10^6 m^3. The delta newly developed after extension of the jetties was first symmetrical owing to the tidal force. Then, as the delta developed and the water depth over the delta decreased, the influence of waves on the sediment movement increased. As a result, the delta became skewed. Long-term bathymetric change around St. Marys Entrance, a tidal inlet with jetties in Florida, USA, was examined by KNOWLES and GORMAN (1991) and BYRNES and HILAND (1995). The mean spring tidal range is 2.1 m, and the tidal prism is about 200 $\times$ 10^6 m^3. KNOWLES and GORMAN (1991) calculated volumetric changes in the vicinity of the jetties with bathymetric data obtained in 1924 and 1970's to estimate the gross and the net longshore sediment transport rates. Moreover, they showed the significant short-term bathymetric change af-

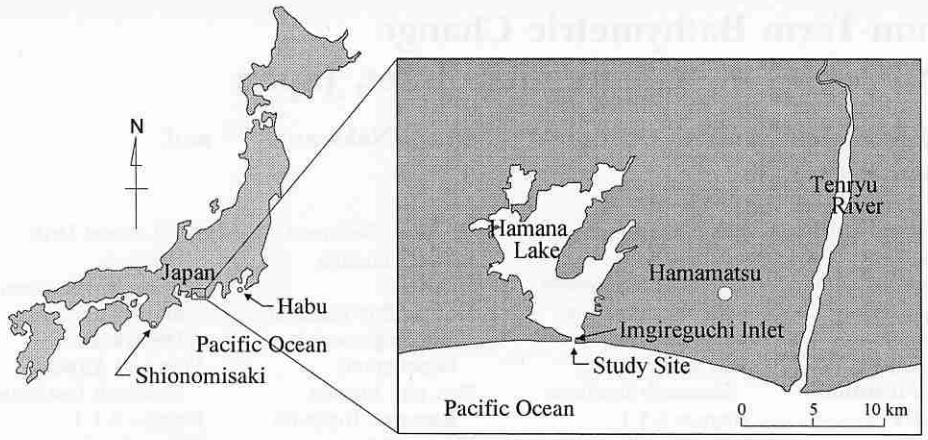

Figure 1. Location of Imagireguchi Inlet.

ter construction of the jetties followed by the long-term moderate morphological change. BYRNES and HILAND (1995) conducted a comprehensive investigation on the bathymetric change and the sediment transport along the coast where St. Mary's Entrance is located, and demonstrated that sediments on the ebb-tidal delta created before construction of the jetties were transported seaward after construction of the jetties, and formed a new ebb-tidal delta in deeper water, which resulted in the decrease of the amount of sediment bypassing around the delta.

The sediment budget over a tidal inlet with jetties, Shinnecock Inlet in New York, USA, was investigated by KANA (1995). One of the results indicates that the net sediment transport rate reduces from 220,000 m^3/yr on the up-drift side of the jetties to 104,000 m^3/yr on the down-drift side implying that about half of the sediment transported alongshore is trapped by the jetties and the inlet system. TOMIYA *et al.* (1987) investigated the longshore sediment transport rate through Imagireguchi Inlet in Japan, the study site in this paper, with survey data obtained during 1963 and 1985 to conclude that the direction of the predominant longshore sediment transport is westward and the net longshore sediment transport rate is about 120,000 m^3/yr.

LIU and HOU (1997) analyzed about 200 samples of sediment on the bottom taken in and around a tidal inlet with breakwaters, Kaoshiung Harbor in Taiwan, where the tidal range varies from 0.7 m to 1.7 m. They found that there were four types of sediment transport around the breakwaters, and the types were determined by the sediment diameter. Most of the medium and coarse sediments, of which the diameter ranges from 0.25 mm to 1 mm, were transported to the down-drift beach by bypassing around the breakwaters.

The objective of this study is to investigate medium-term bathymetric changes induced by construction of jetties at the entrance of a tidal inlet with a 30-year extensive bathymetric data set. The data set is analyzed by empirical orthogonal eigenfunction analysis and complex empirical orthogonal eigenfunction analysis.

STUDY SITE

The study area is Imagireguchi Inlet in Japan, which connects the Pacific Ocean with Hamana Lake having an area of 74 km^2; the location is shown in Figure 1. The tidal range is 1.4 m, and the high, the mean and the low water levels based on the datum level are 1.4 m, 0.7 m and 0.0 m, respectively. The tidal prism is about 20×10^6 m^3 (MAZDA, 1983). According to long-term wave data measured at Shionomisaki and Habu (NAGAI *et al.*, 1993), of which the locations are shown in Figure 1, the mean significant wave height and period offshore of Imagireguchi Inlet are expected to be about 1.3 m and 7.3 s. The sediment diameter ranges from 0.2 mm to 0.3 mm.

Because Imagireguchi Inlet was unstable and was a concern for navigation, two jetties were constructed for stabilization of the navigation channel

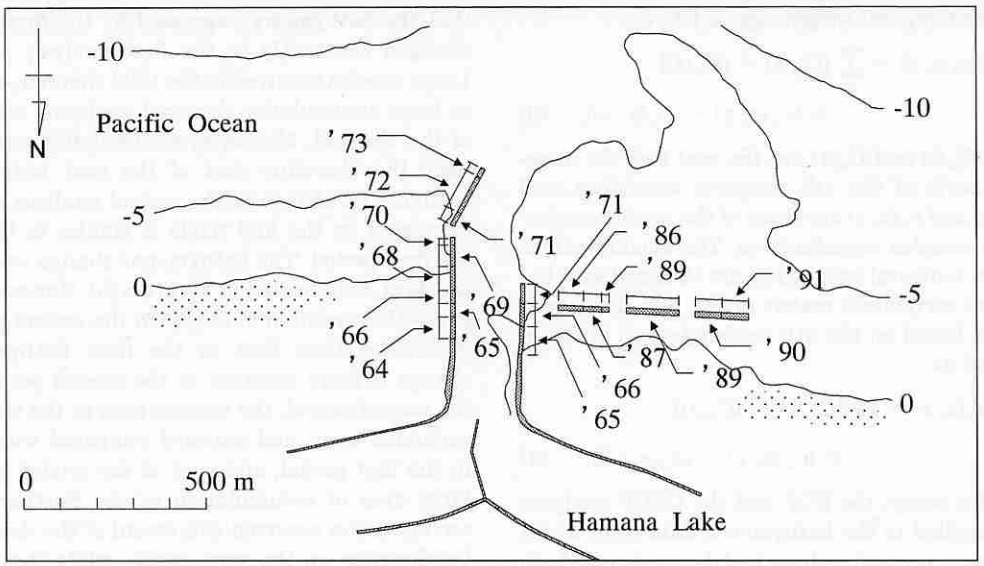

Figure 2. History of the construction of coastal structures with bathymetric contours based on the datum level in 1992.

(MAZDA, 1983). Construction of the jetties started in 1954, and the first stage was completed in 1970. Then, the east jetty was expanded between 1971 and 1973. West of the west jetty, three detached breakwaters were constructed. The history of the construction of the coastal structures is shown in Figure 2 with bathymetric contours in 1992.

FIELD DATA AND ANALYSIS METHODS

Field surveys were conducted almost every year in the area about 2,000 m alongshore and about 1,200 m across shore, where bathymetric contours are shown in Figure 2, and the survey areas slightly differed with survey dates. The alongshore and cross-shore spacing of the survey points is 50 m.

The survey data were analyzed with empirical orthogonal eigenfunction (EOF) analysis and complex empirical orthogonal eigenfunction (CEOF) analysis. EOF analysis can identify patterns of simultaneous variation (VON STORCH and ZWIERS, 1999), and is useful to compress the complicated variability of the original data set into the fewest possible number of modes (HOREL, 1984). Hence, it has been widely applied to the analysis of morphological data (*e.g.* WINANT *et al.*, 1975; AUBREY, 1979; BIRKEMEIER, 1984; WIJNBERG and TERWINDT, 1995). In the analysis of morphological change, the independent variation patterns are expressed with the products of spatial and temporal functions as

$$z(x, y, t) = \sum_n C_n(t) e_n(x, y), \quad (1)$$

where $z(x, y, t)$ is the elevation, x is the cross-shore coordinate, y is the alongshore coordinate, t is time, $C_n(t)$ is the nth temporal weighting, and $e_n(x, y)$ is the nondimensional nth eigenfunction. Because the vertical axis is defined to extend upward, a positive value of the difference between two products of $C_n(t)$ and $e_n(x, y)$ indicates that the bathymetric change during the period is accumulation.

CEOF analysis is an expanded EOF analysis and has been applied to analyze beach profile data by LIANG and SEYMOUR (1991), RUESSINK *et al.* (2000), and KURIYAMA and LEE (2001). EOF analysis is limited to detecting standing waves, whereas CEOF has the advantage of detecting propagating waves.

As in LIANG and SEYMOUR (1991) and RUESSINK *et al.* (2000), time series of the variation of elevation $z(x, y, t)$ is first transformed into a complex data set $Z(x, y, t)$ as

$$Z(x, y, t) = z(x, y, t) + i\hat{z}(x, y, t) \quad (2)$$

where $\hat{z}(x, y, t)$ is the Hilbert transform of $z(x, y, t)$.

Then, $Z(x, y, t)$ is divided into products of the

nondimensional complex eigenfunctions and the complex temporal weightings as follows:

$$Z(x, y, t) = \sum_n [C_{nr}(t) + iC_{ni}(t)] \times [e_{nr}(x, y) - ie_{ni}(x, y)], \quad (3)$$

where $C_{nr}(t)$ and $C_{ni}(t)$ are the real and the imaginary parts of the nth temporal weighting, and $e_{nr}(x, y)$ and $e_{ni}(x, y)$ are those of the nondimensional nth complex eigenfunction. The eigenfunctions and the temporal weightings are obtained with the complex correlation matrix of $Z(x, y, t)$. The beach process based on the nth mode $z_n(x, y, t)$ is reconstructed as

$$z_n(x, t) = \mathrm{Re}\{[C_{nr}(t) + iC_{ni}(t)] \times [e_{nr}(x, y) - ie_{ni}(x, y)]\}. \quad (4)$$

In this study, the EOF and the CEOF analyses were applied to the bathymetric data from which the time-averaged values had been removed. In addition to the two analyses, volumetric changes in the investigation area were also analyzed.

RESULTS

Figure 3 shows aerial photographs of Imagireguchi Inlet taken in 1969 and 1991. The left figures of Figures 4 (1) and (2) show bathymetric contours in 1963, 1967, 1972, 1980, 1987 and 1992, and the right figures show contours for bathymetric changes. In 1963, just after the start of construction of the jetties, an ebb-tidal delta developed in front of the inlet and was almost symmetrical with respect to the tidal channel. During a period from 1963 to 1992, accumulation occurred east of the east jetty. Furthermore, the tidal channel deepened, and sediments were accumulated westward of the channel. As a result, the ebb-tidal delta shifted westward, and was skewed in 1992.

To examine the time variation of the influence of the jetties on the bathymetry, we divided the investigation period between 1963 and 1993 into two periods: from 1963 to 1975, during and just after construction of the jetties, and from 1980 to 1993. Then, we applied the EOF analysis to the survey data during two periods. Figure 5 shows the first eigenfunction e_1, the temporal weighting C_1 and the change rate of C_1 with respect to time dC_1/dt in the first period, and Figure 6 shows those in the second period; the variances explained by the first modes in the first and second periods are 32% and 41%, respectively. The time variation of the temporal weighting shown in Figure 5 (b), which increases almost monotonically, indicates that the bathymetry expressed by the first mode changed constantly in the first analysis period. Large erosion occurred in the tidal channel, whereas large accumulation occurred west- and seaward of the channel. Moreover, accumulation occurred near the shoreline east of the east jetty. The bathymetric change in the second analysis period expressed by the first mode is similar to that in the first period. The bathymetric change was also constant as indicated in Figure 6 (b). However, because the variation of dC_1/dt in the second period is smaller than that in the first, bathymetric change is more constant in the second period. In the second period, the erosion area in the channel expanded west- and seaward compared with that in the first period, and west of the eroded area a large area of accumulation exists. Furthermore, accumulation occurred shoreward of the detached breakwaters on the west beach, while the beach located east of the east jetty was eroded near the shoreline.

According to the characteristics of the bathymetric change shown by the results of the first modes in the EOF analysis (Figures 5 and 6), the investigation area was divided into nine areas, shown in Figure 7. Polygons A, B and C are located in the up-drift side, east of the east jetties. Polygons A and C correspond to the areas where accumulation occurred in the first modes, whereas polygon B corresponds to the area where erosion occurred. Polygon D includes the tidal channel, and covers the area where erosion occurred in the first modes. The region seaward of the detached breakwaters, where accumulation occurred in the first modes, was divided into three areas, polygons F, G and H, based on the cross-shore distance. Polygons E and I are located shoreward and westward of the breakwaters, respectively. Figure 8 shows the time series of the volumes in the nine areas. The volume in polygon H is based on that in 1973, and the other volumes are based on those in 1963.

Table 1 shows the accumulation rates in the nine areas during the two analysis periods estimated with the least square method. As shown in Table 1, in polygons A, B and C, east of the east jetty, the accumulation rates decreased. On the other hand, in polygons E, F, and G, the accumulation rates increased. In polygon D, where the channel is located, the erosion rate increased. The total volumes of sediment accumulated in the in-

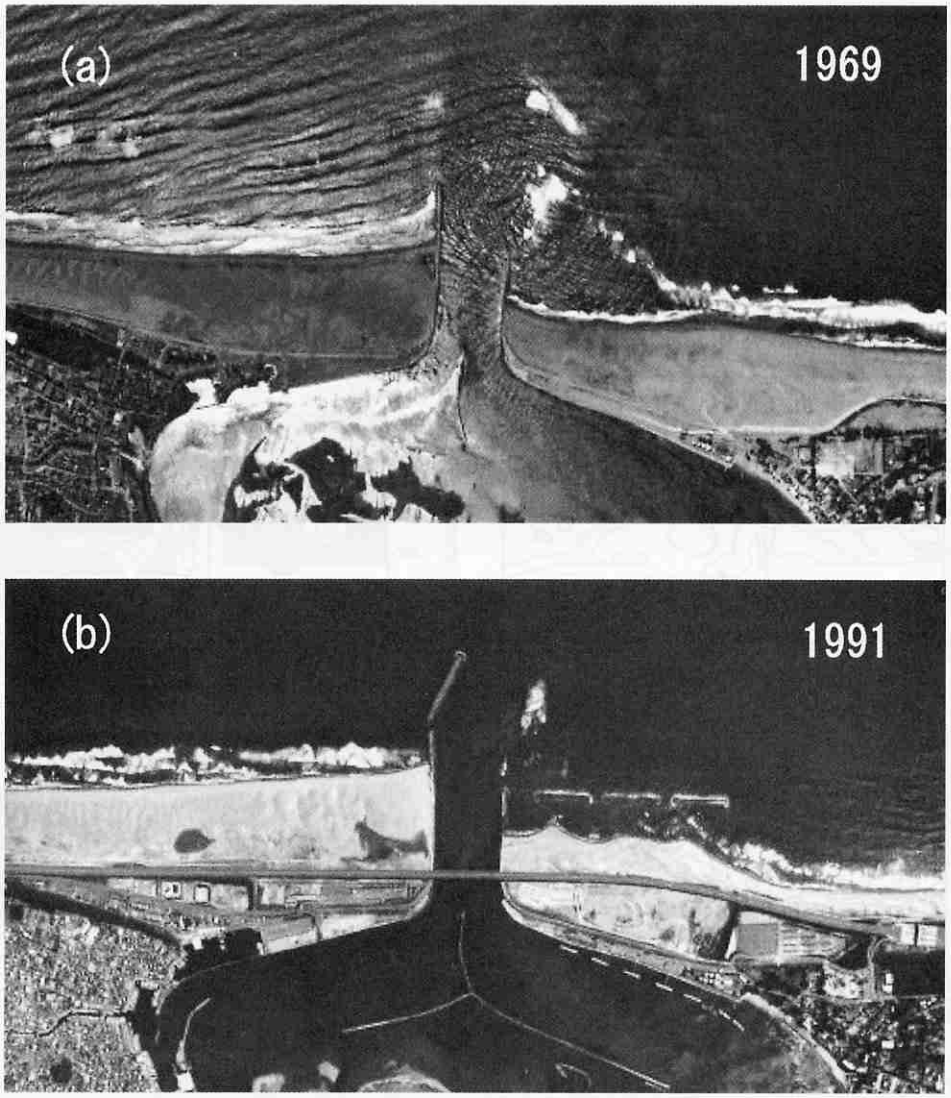

Figure 3. Aerial photographs of Imagireguchi Inlet taken in 1969 and 1991.

vestigation area except for polygon H are almost the same in the two analysis periods.

As shown in Figure 8 (b), accumulations started with time lags in the order of polygons H, G, F, and I. This order of accumulation indicates that sediment was first deposited on the west- and seaward edge of the delta, and then the accumulation area expanded west- and shoreward.

To examine the influence of the jetties on bathymetric changes with propagating features such as bar movement, we applied the CEOF analysis. Figure 9 shows the results of the first mode in the first period, and Figure 10 shows those in the second period; the variances explained by the first modes in the two periods are 43% and 50%, respectively. The bathymetric changes during the two periods expressed by the first modes in the CEOF analysis are similar to those expressed by the first modes in the EOF analysis. Both in the first and the second periods, the imaginary parts of the first eigenfunctions and those of the temporal weightings in the CEOF analysis are similar

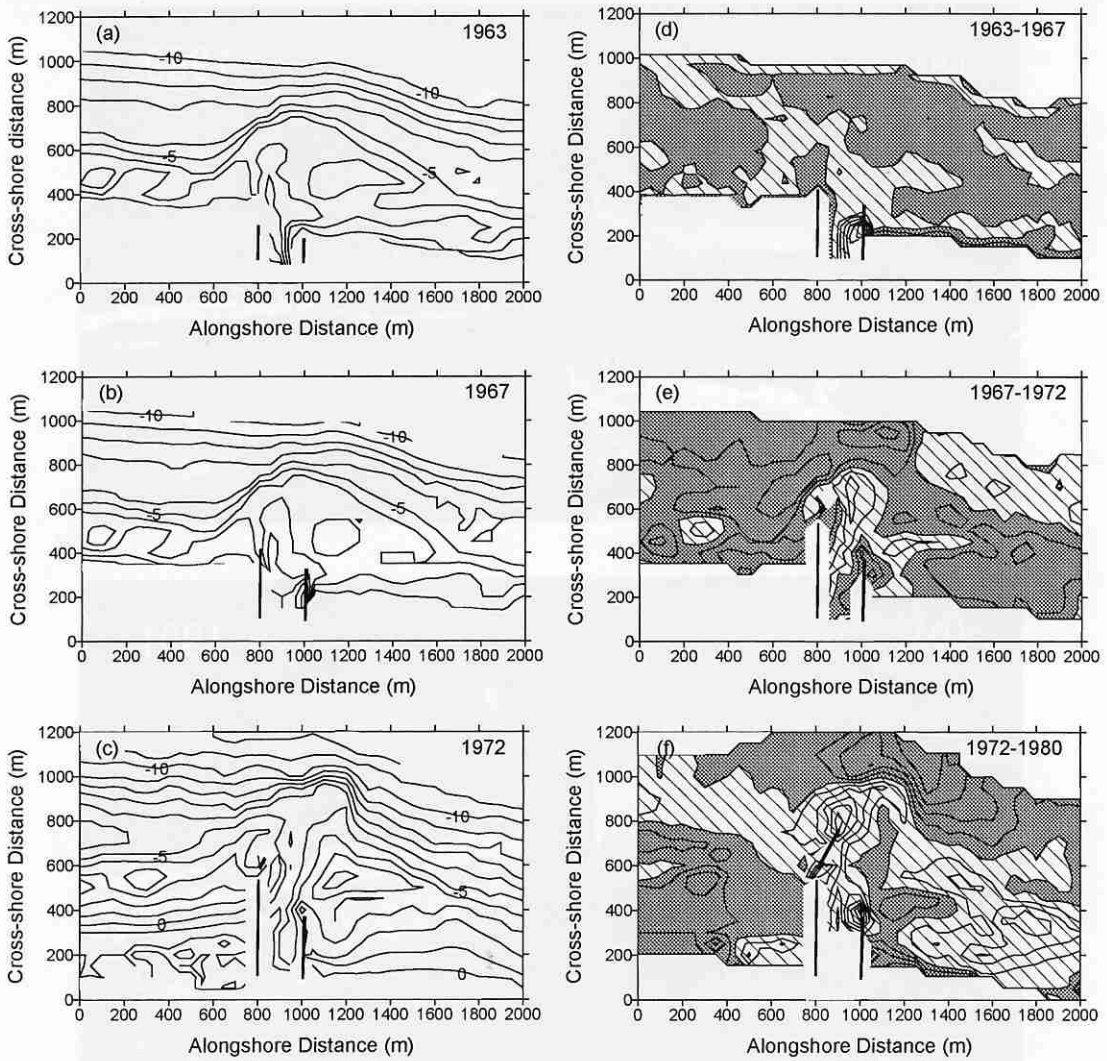

Figure 4(1). (a)–(c) Bathymetric contours in 1963, 1967 and 1972. The contour interval is 1 m. (d)–(f) Contours for bathymetric changes during periods from 1963 to 1967, from 1967 to 1972, and from 1972 to 1980. The accumulated and eroded areas are shown by gray color and slash, respectively. White color indicates no data. The contour interval is 1 m.

to the first eigenfunctions and the temporal weightings in the CEOF analysis (Figures 5 and 6), respectively. Similarly, the real parts of the first eigenfunctions and the temporal weightings are almost the same as the second eigenfunctions and the temporal weightings in the EOF analysis, which are not presented in the text. The result that the real and imaginary parts of the first complex eigenfunction in the CEOF analysis and those of the complex temporal weighting are similar to the first and second eigenfunctions in the EOF analysis and the temporal weightings was also found by KURIYAMA and LEE (2001).

Although the first modes in the CEOF analysis show the bathymetric changes similar to those expressed by the first modes in the EOF analysis, the first modes in the CEOF analysis express the movements of accumulation and erosion areas. Figure 11 shows the bathymetric changes during periods from 1964 to 1967, and from 1970 to 1974 obtained on the basis of the bathymetries reconstructed with the first mode in the CEOF analysis.

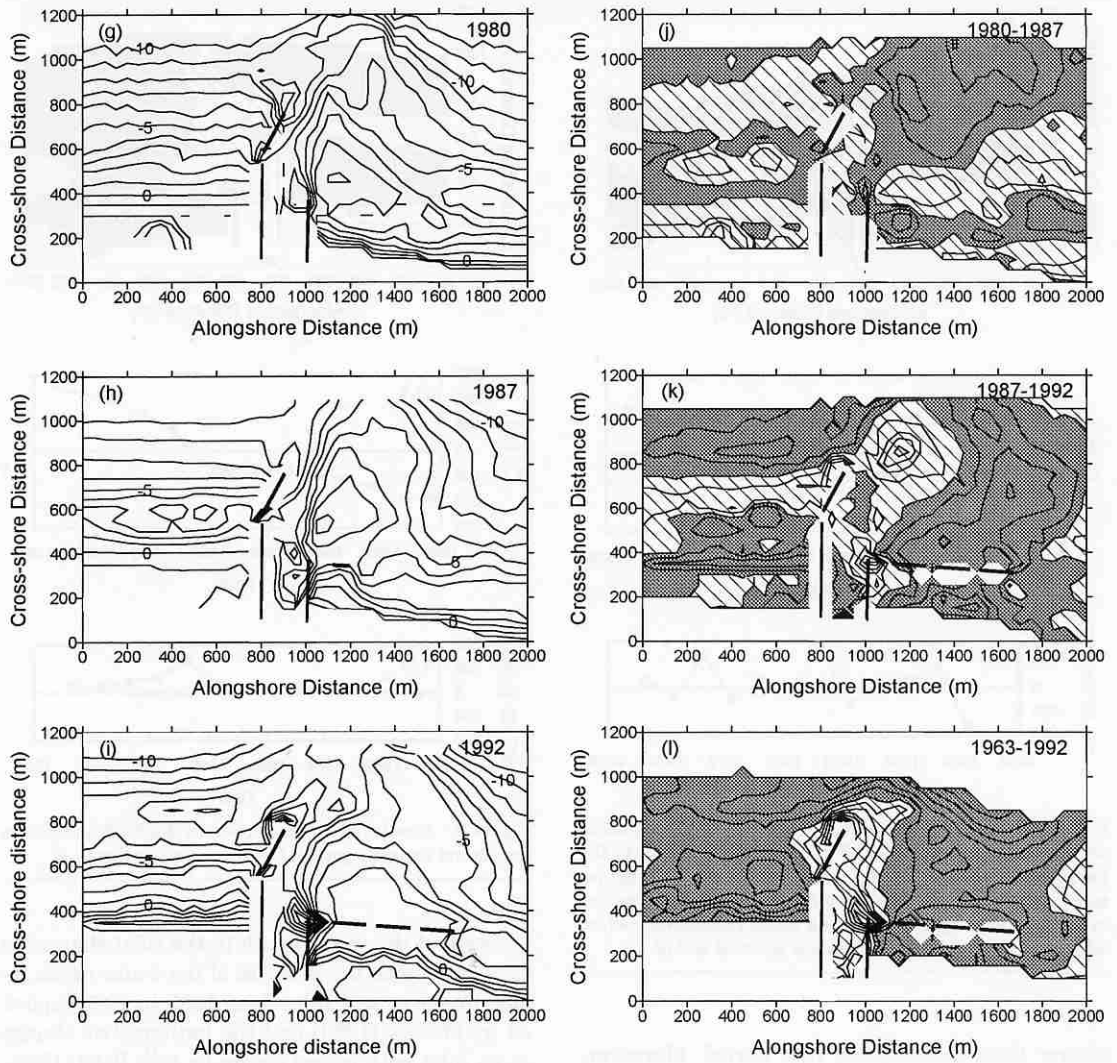

Figure 4(2). (g)–(i) Bathymetric contours in 1980, 1987 and 1992. (j)–(l) Contours for bathymetric changes during periods from 1980 to 1987, from 1987 to 1992, and from 1963 to 1992. Details are as in Figure 4 (1).

Figure 12 shows those during periods from 1981 to 1985, and from 1989 to 1992. The erosion area during a period from 1964 to 1967 near the shoreline on the both sides of the inlet shifted seaward during a period from 1970 to 1974. In the second analysis period, west of the jetties, accumulation area moved westward. This movement is also observed in the volumetric changes in polygons H, G, F and I, shown above.

The results of the second modes in the CEOF analysis in the first and the second periods are shown in Figures 13 and 14, respectively; the variances explained by the second modes in the first and second periods are 21% and 18%, respectively. Figure 15 shows the bathymetries expressed by the second mode in 1967, in 1970 and in 1972. Figure 16 shows those in 1987, in 1989 and in 1991. In the first analysis period, areas where elevations are positive and above the time-averaged bathymetry, shoals in the second mode, formed on both sides of the jetties and moved shoreward. In the second period, the movements of the shoals were

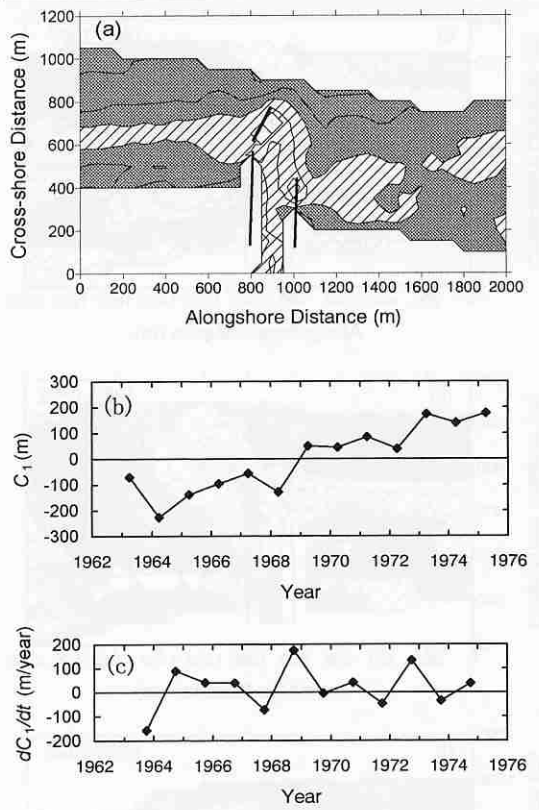

Figure 5. Results of the first mode in the EOF analysis in the first analysis period. (a) First eigenfunction, e_1, (b) the temporal weighting, C_1, and (c) change rate of C_1 with respect to time, dC_1/dt. The positive and the negative values in (a) are shown by gray color and slash, respectively; white color indicates no data. The contour interval is 0.05.

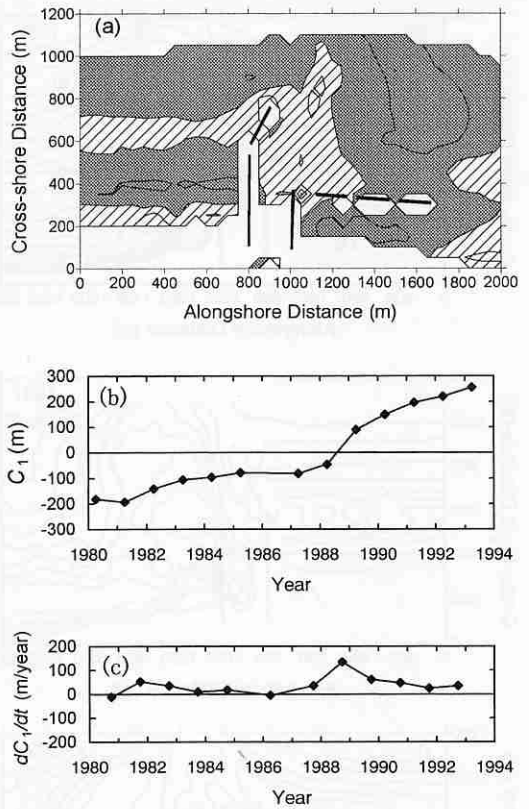

Figure 6. Results of the first mode in the EOF analysis in the second analysis period. Details are as in Figure 5.

clearer than those in the first period. Moreover, although the shoal west of the west jetty moved shoreward as schematically shown by ROSATI and KRAUS (2001), the shoal on the east side moved seaward. On the basis of the variations of the temporal weightings in the second mode in the CEOF analysis, shown in Figures 13 (c) and 14 (c), the periods of the shoal movements are estimated to be 8 to 10 years, which is a little longer that that of 5 to 7 years reported by FITZGERALD (1982) for the Popham Beach, Maine, USA.

DISCUSSION

As shown in Table 1, in polygon D, where the tidal channel is located, erosion occurred and the erosion rate increased. The erosion indicating the increase of the water depth in the tidal channel is consistent with the increase of the water depth inside Imagireguchi Inlet from 1960 to 1980 reported by MAZDA (1983) and the bathymetric change at an inlet with jetties shown by VAN RIJN (1998).

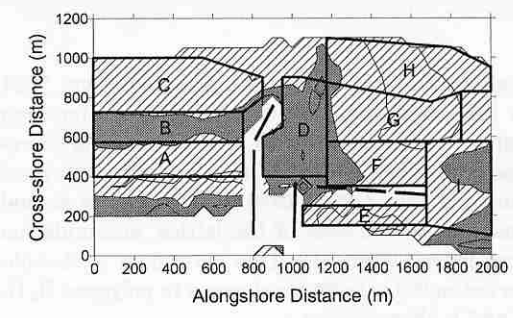

Figure 7. Locations of nine areas with e_1 in the EOF analysis in the second analysis period. Details are as in Figure 5.

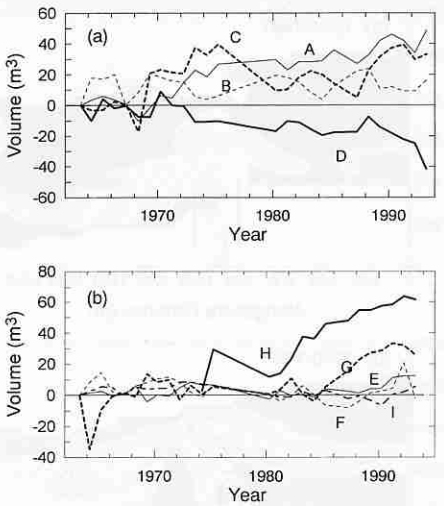

Figure 8. Volumetric changes (a) in polygons A–D and (b) in polygons E–I.

The increase in the erosion rate in the channel is probably caused by the stabilization of the location of the channel by the jetties, and focusing of the ebb jet between the jetties. When the location of a tidal channel is unstable, an area in front of the inlet experiences both accumulation and erosion. When the location of the channel is fixed, however, the area where the channel is located is always exposed to the tidal current. As a result, the channel deepens to some equilibrium depth. This interpretation is supported by the results of the first modes in the EOF analysis. As shown in Figures 5 (c) and 6 (c), the variation of dC_I/dt in the second period, from 1980 to 1993, is smaller than that in the first period, from 1963 to 1975.

Table 1. *Accumulation rates ($\times 10^3$ m³/year).*

Area	1963–1975	1980–1993
A	20.1	14.6
B	−3.0	−2.1
C	39.9	19.4
D	−5.7	−11.9
E	5.4	9.8
F	−0.8	5.8
G	16.2	27.4
H	—	38.9
I	4.9	0.6
A + B + C	57.0	31.9
F + G	15.4	33.2
Total (except for H)	77.0	63.6

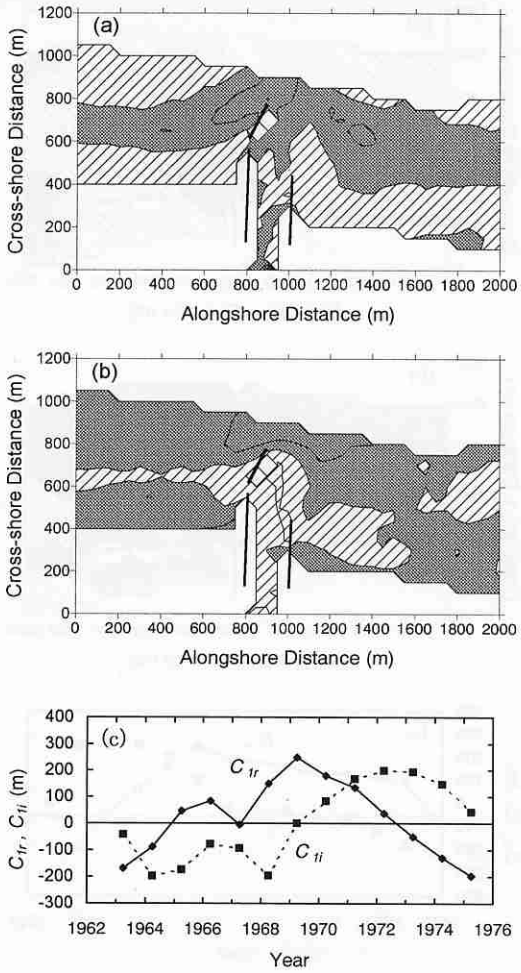

Figure 9. Results of the first mode in the CEOF analysis in the first analysis period. (a) Real part of the first eigenfunction, e_{1r}, (b) imaginary part of the first eigenfunction, e_{1i}, and (c) real and imaginary parts of the temporal weighting, C_{1r} and C_{1i}. The positive and the negative values in (a) and (b) are shown by gray color and slash, respectively. White color indicates no data. The contour interval in (a) and (b) is 0.05.

This means that the bathymetric change was more constant in the second period as compared to the first, and indicates that the location of the tidal current was more stable in the second period than in the first.

The reason of the decrease in the accumulation rate on the east side, the up-drift side of the jetties, shown in Table 1, is considered to be that the bathymetry on the east side reached close to equilibrium. The decrease in the accumulation rate on

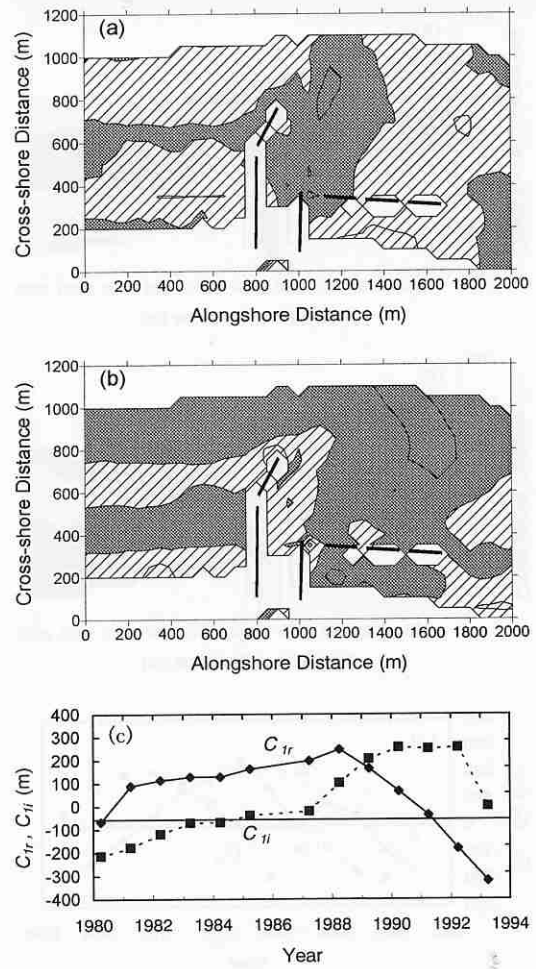

Figure 10. Results of the first mode in the CEOF analysis in the second analysis period. Details are as in Figure 9.

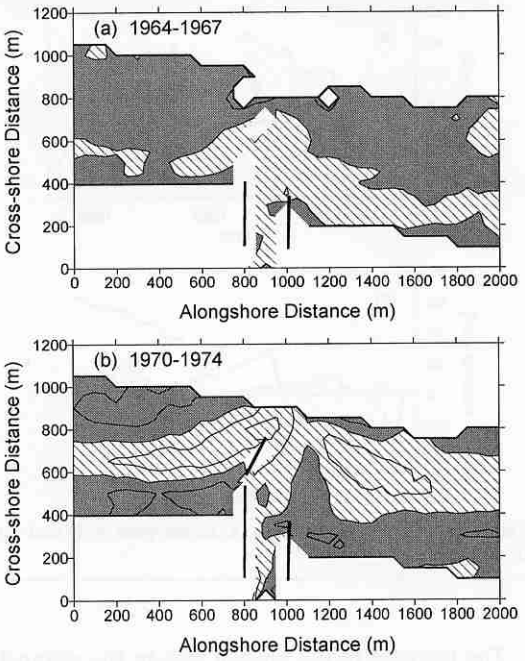

Figure 11. Bathymetric changes during periods from 1964 to 1967, and from 1970 to 1974 obtained on the basis of the bathymetries reconstructed with the first mode in the first period in the CEOF analysis. The accumulated and the eroded areas are shown by gray color and slash, respectively. The contour interval is 1 m.

the up-drift side was also observed by TOMLINSON (1991).

The decrease in the accumulation rate on the east side results in the increase of the amount of sediment passing around the jetties and supplied to the west side of the jetties. Consequently, the amount of sediment accumulated on the west side increased, whereas the increase is partially due to the increase in the erosion rate in the tidal channel. As a result, the total amount of sediment trapped in the study area is almost constant in the first and second analysis periods. This result indicates that the amount of sediment supplied to the down-drift beach does not increase immediately after the bathymetry on the up-drift side of the jetties reaches equilibrium, and that the influence of a jetty at a tidal inlet on the bathymetric change is different from that of a groin on a sandy beach. When the bathymetry on the up-drift side of a groin is close to equilibrium, the amount of sediment transported around the groin is expected to increase. Consequently, the amount of sediment supplied to the down-drift beach increases. In the vicinity of an inlet with a jetty, however, sediment passing around a jetty is trapped by the ebb-tidal delta until some equilibrium is achieved. As a result, the amount of sediment supplied to the down-drift beach does not increase for a long time period.

The influence of the flood shoal, located landward of the study area, on the sediment budget is not clear. Nevertheless, according to VAN RIJN (1998), the influence is likely to be small because the tidal range at the study site, 1.4 m, is classified in micro-tidal condition, where the ebb current does not have strong power to transport sediments on a flood shoal.

WALTON and ADAMS (1976) showed that the vol-

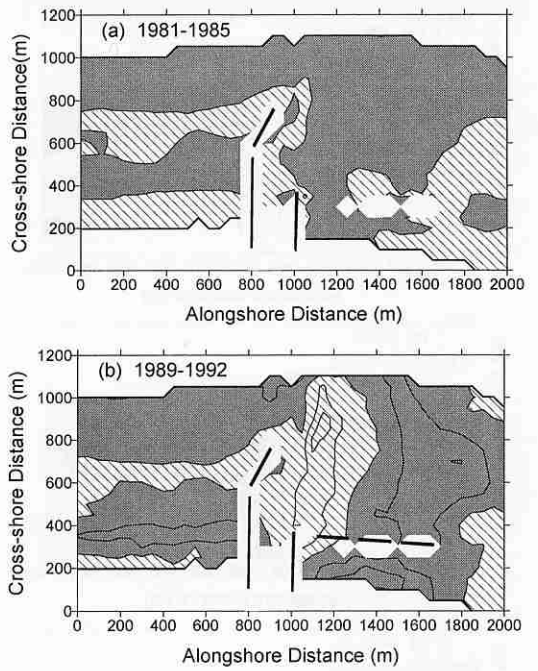

Figure 12. Bathymetric changes during periods from 1981 to 1985, and from 1989 to 1992 obtained on the basis of the bathymetries reconstructed with the first mode in the second period in the CEOF analysis. Details are as in Figure 11.

ume of sediment stored in an ebb-tidal delta has strong correlation with the tidal prism, and the relationship at the exposed coast is expressed as

$$V = 0.0053P^{1.23}, \quad (5)$$

where V is the volume of sediment stored in an ebb-tidal delta in cubic meters and P is the tidal prism in cubic meters. The mean significant wave height H and period T in the study coast are 1.3 m and 7.3 s, as shown above, and thus the study coast, where H^2T^2 is about 90 m^2s^2, is categorized in the exposed coast ($H^2T^2 > 30$ m^2s^2).

The volume of sediment stored in the ebb-tidal delta was estimated on the basis of the natural bathymetry of the coast without the inlet. As in WALTON and ADAMS (1976), the natural bathymetry was obtained with natural beach profiles that are not affected by the inlet; the profiles measured in 1963 at the side boundaries of the study area, where the alongshore distance is 0 and 2000 m, were assumed to be natural. The shoreline positions of the natural bathymetry were interpolated with those of the boundaries, and the beach profiles along the surveying lines were set to be the mean beach profile of those at the boundaries. The elevations shoreward and seaward of the mean beach profile were extrapolated.

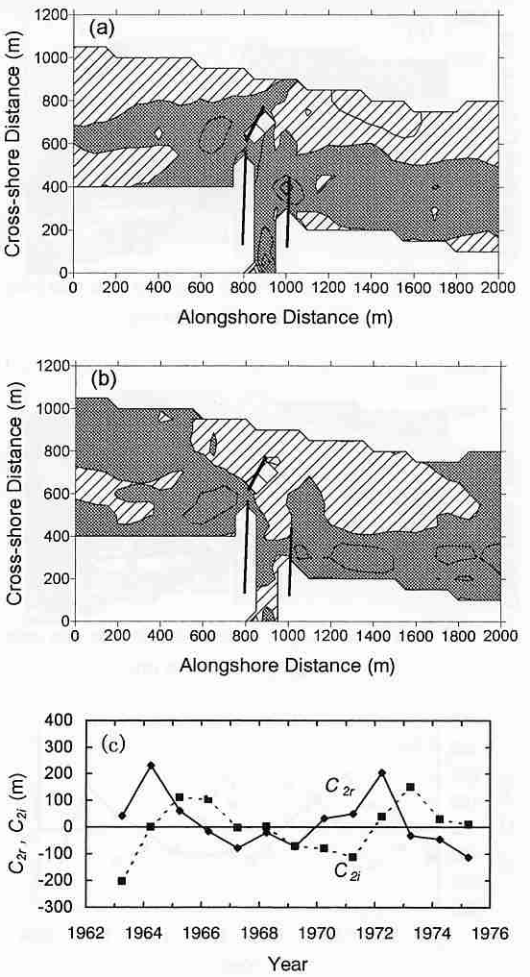

Figure 13. Results of the second mode in the CEOF analysis in the first analysis period. (a) Real part of the second eigenfunction, e_{2r}, (b) imaginary part of the second eigenfunction, e_{2i}, and (c) real and imaginary parts of the temporal weighting, C_{2r} and C_{2i}. The positive and the negative values in (a) and (b) are shown by gray color and slash, respectively. White color indicates no data. The contour interval in (a) and (b) is 0.05.

The contour map of the estimated natural bathymetry is shown in Figure 17 with that of the bathymetry measured in 1992. The volume of sediment stored in the study area in 1992 is about 4,300,000 m^3. The equilibrium volume of sediment

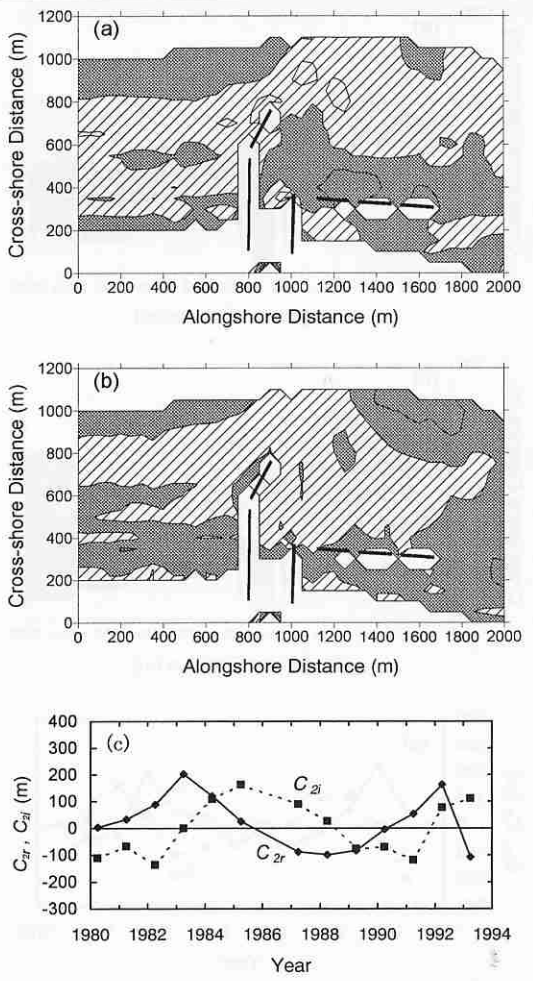

Figure 14. Results of the second mode in the CEOF analysis in the second analysis period. Details are as in Figure 13.

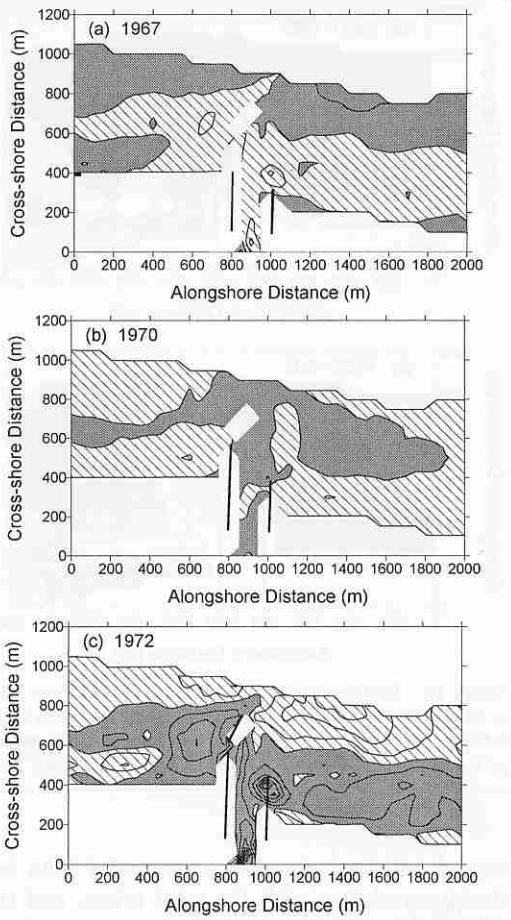

Figure 15. Bathymetries in 1967, 1970 and 1972 reconstructed with the second eigenfunction and the temporal weighting in the first period in the CEOF analysis. The positive and the negative values are shown by gray color and slash, respectively. White color indicates no data. The contour interval is 0.5 m.

stored in the ebb-tidal delta estimated with Eq. (5) is about 5,000,000 m^3. Considering that the study area does not cover the whole ebb-tidal delta, the volume of sediment stored in the ebb-tidal delta is assumed to reach close to the equilibrium. This is consistent with the result that the accumulation area created first at the west- and seaward edge of the tidal-delta moved west- and shoreward, and almost reached the shoreline of the down-drift beach, as shown in Figure 12 (b).

The bathymetries reconstructed by the second modes in the CEOF analysis (Figures 15 and 16) showed that shoals formed on the both sides of the jetties and moved shoreward in the first period. In the second period, however, although the shoal west of the west jetty, on the down-drift side, moved shoreward, the shoal on the up-drift side moved seaward. FITZGERALD (1982) reported the shoreward shoal movement at an inlet without coastal structures and deduced that the shoreward shoal movement was caused by flood tides and waves. At Imagireguchi Inlet, after extension of the east jetty, the tidal current became weaker east of the east jetty. That resulted in the dominance of the seaward return flow and the westward wave-generated longshore current, which changed the direction to offshore in the vicinity of

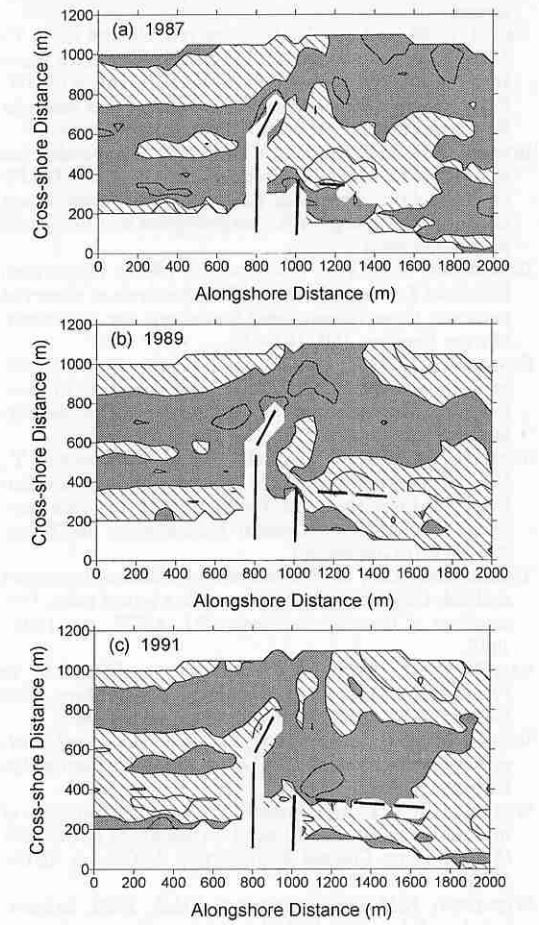

Figure 16. Bathymetries in 1987, 1989 and 1991 reconstructed with the second eigenfunction and the temporal weighting in the second period in the CEOF analysis. Details are as in Figure 15.

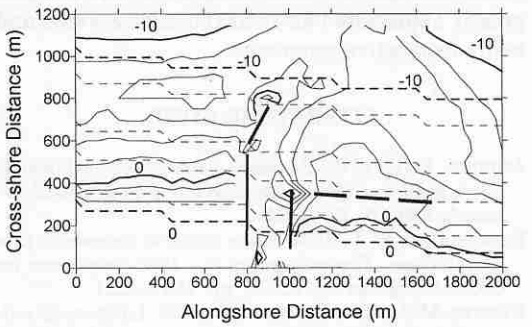

Figure 17. Bathymetric contours for the natural bathymetry (broken lines) and those in 1992 (solid lines). The contour interval is 2 m.

the east jetty similar to the longshore current frequently measured on the up-drift side of a groin (*e.g.*, SAWARAGI, 1995). The return flow and the wave-generated longshore current probably caused the seaward shoal movement.

CONCLUSIONS

A 30-year bathymetric data set obtained during and after construction of jetties at an entrance of Imagireguchi Inlet was analyzed. After construction of the jetties, the tidal channel deepened. Moreover, the erosion rate in the channel increased. The increase in the erosion rate is probably caused by the stabilization of the location of the channel, which had the area including the channel always exposed to the tidal current, and focusing of the ebb jet between the jetties.

Although accumulation occurred on the up-drift side of the jetties, the accumulation rate decreased with time. However, the amount of sediment supplied to the down-drift beach did not increase because some amount of sediment transported around the jetties was trapped to develop the ebb-tidal delta. The volume stored in the ebb-tidal delta was estimated, and compared with the equilibrium one calculated using the relationship between the equilibrium volume and the tidal prism proposed by WALTON and ADAMS (1976). The comparison showed that the volume almost reached the equilibrium.

In the first analysis period, during and just after construction of the jetties, shoals formed on both sides of the jetties and moved shoreward. In the second period, however, although the shoal on the down-drift side moved still shoreward, the shoal on the up-drift side moved seaward. This is because the east jetty reduced the influence of the tidal current east of the east jetty, on the up-drift side. As a result, the seaward return flow and the wave-generated westward longshore current, which turned the direction and flowed seaward at the east jetty, became predominant and caused seaward movement of the shoal east of the east jetty.

ACKNOWLEDGEMENTS

We are grateful to Ms. Mayumi Fujii for her help in analyzing the bathymetric data, which were provided by Sizuoka Prefecture. Dr. Kazumasa

Katoh and the two anonymous reviewers are also greatly appreciated for their thorough reviews and many instructive comments.

LITERATURE CITED

AUBREY, D.G., 1979. Seasonal patterns of onshore/offshore sediment movement. *Journal of Geophysical Research,* 84(C10), 6347–6354.

BIRKEMEIER, W.A., 1984. Time scales of nearshore profile changes. *Proceedings of the 19th Conference on Coastal Engineering,* ASCE, pp. 1507–1521.

BYRNES, M.P. and HILAND, M.W., 1995. Large-scale sediment transport patterns on the continental shelf and influence on shoreline response: St. Andrew Sound, Georgia to Nassau Sound, Florida, USA. *Marine Geology,* 126, 19–43.

FITZGERALD, D.M., 1982. Sediment bypassing at mixed tidal inlets. *Proceedings of the 18th Conference on Coastal Engineering,* ASCE, pp. 1094–1118.

HOREL, J.D., 1984. Complex principal component analysis: theory and examples. *Journal of Climate and Applied Meteorology,* 23, 1600–1673.

KANA, T.W., 1995. A mesoscale sediment budget for Long Island, New York. *Marine Geology,* 126, 87–110.

KNOWLES, S.C. and GORMAN, L.T., 1991. Historical coastal morphodynamics at St. Marys entrance and vicinity, Florida, USA. *Proceedings of Coastal Sediments '91,* ASCE, pp. 1447–1461.

KURIYAMA, Y. and LEE, J.H., 2001. Medium-term beach profile change on a bar-trough region at Hasaki, Japan, investigated with complex principal component analysis. *Proceedings of Coastal Sediments '01,* ASCE, pp. 959–968.

LIANG, G. and SEYMOUR, R., 1991. Complex principal component analysis of wave-like sand motions. *Proceedings of Coastal Sediments '91,* ASCE, pp. 2175–2186.

LIU, J.T. and HOU, L.H., 1997. Sediment trapping and bypassing characteristics of a stable tidal inlet at Kaohsiung Harbor, Taiwan. *Marine Geology,* 140, 367–390.

MAZDA, Y., 1983. Oceanographic environment in Lake Hamana—Year-to-year variation of tidal condition induced by topographic change of lake mouth. *Bulletin on Coastal Oceanography,* 20(2), pp. 178–188. (in Japanese)

NAGAI, T.; SUGAHARA, K.; HASHIMOTO, N., and ASAI, T., 1993. 20-year statistics of the Nationwide Ocean Wave Information Network for Ports and Harbours (NOWPHAS) 1970–1989. *Technical Note of Port and Harbour Research Institute, No. 744,* 247 p. (in Japanese)

ROSATI, J.D. and KRAUS, N.C., 2000. Shoal-reduction strategies for entrance channels, *ERDC/CHL TN-IV-22,* U.S. Army Engineer Research and Development Center, Vicksburg, MS. http://bigfoot.wes.army.mil/cetn.index.html

RUESSUNK, B.G.; VAN ENCKEVORT, I.M.J.; KINGSTON, K.S., and DAVIDSON, M.A., 2000. Analysis of observed two- and three-dimensional nearshore bar behaviour, *Marine Geology,* 169, 161–183.

SAWARAGI, T., 1995. *Coastal engineering—Waves, beaches, wave-structure interactions,* Development in Geotechnical Engineering, 78. Amsterdam, The Netherlands: Elsevier. 479 p.

TOMIYA, T.; UDA, T.; SAKAI, Y., and YAMAMOTO, T., 1987. Topographic changes around jetties at the Entrance of Lake Hamana, *Proceedings of the 34th Japanese Conference on Coastal Engineering,* JSCE. pp. 367–371. (in Japanese)

TOMLINSON, R.B., 1991. Processes of sediment transport and ebb tidal delta development at a jetted inlet. *Proceedings of Coastal Sediments '91,* ASCE, pp. 1404–1418.

VAN RIJN, L.C., 1998. Sand Coast. *In*: van Rijn, L.C., in *Principles of coastal morphology.* Amsterdam, The Netherlands: Aqua Publications. pp. 4.1–4.540.

VON STORCH, H. and ZWIERS, F., 1999. *Statistical analysis in climate research.* Cambridge, UK: Cambridge University Press. 484 p.

WALTON, JR. T.L. and ADAMS, W.D., 1976. Capacity of inlet outer bars to store sand. *Proceedings of the 15th Conference on Coastal Engineering,* ASCE, pp. 1919–1937.

WIJNBERG, K.M. and TERWINDT, J.H.J., 1995. Extracting decadal morphological behaviour from high-resolution, long-term bathymetric surveys along the Holland coast using eigenfunction analysis. *Marine Geology,* 126, 301–330.

WINANT, D.C.; INMAN, D.L., and NORDSTROM, C.E., 1975. Description of seasonal beach changes using empirical eigenfunction, *Journal of Geophysical Research,* 80(15), pp. 1979–1986.